Optimized Theoretical Analysis of Antimony Selenide (Sb_2Se_3) Chalcogenide Thin Film

Emmanuel Ifeanyi Ugwu
Department of Industrial Physics, Ebonyi State University, P.M.B 53. Abakaliki, Nigeria

Abstract— Theoretical analysis of the optical and Solid State properties of Antimony Selenide (Sb_2Se_3) thin film using beam propagation technique in which a scalar wave is propagated through the material thin film deposited on a substrate with the assumption that the dielectric medium is section into a homogenous reference dielectric constant term, ε_{ref} and a perturbed dielectric term, $\Delta\varepsilon_p(r)$ representing the deposited thin film medium is presented in this work. These two terms, constitute arbitrary complex dielectric function that describes dielectric perturbation imposed by the medium for the system. This is substituted into a defined scalar wave equation in which the appropriate Green's Function was defined on it and solved using series technique. The field value obtained from Green's Function was used in computation the propagated fields for different wavelength within three windows of electromagnetic wave spectrum during which the influence of the dielectric constants of Sb_2Se_3 thin film on the propagating field was considered. The results obtained from the computation were used in turn to obtain the data that were used in turn to compute the band gaps, solid state and optical properties of the thin film such as reflectance, Transmittance, reflectance and band gap of the thin film.

1. INTRODUCTION

Antimony selenide (Sb_2Se_2) amorphous crystalline thin film (Sato and Miyaoka, 1983) is an alternative material due to its unique switching photovoltaic, thermoelectric, optical and electrical properties [1–3]. Based on this, researchers on material and nona scientists have veraciously applied various techniques to synthesize Sb_2Se_3 thin film. Such methods were single source precursor [4], electro-deposition [4], high temperature evaporation [5] coupled with the use of solution growth technique [7]. In each of these methods, the desire was to discover the one that could be found to enhance optimum efficiency and stabilities in photoelectochemical solar cell configuration as prefigured by [12] that sulfide and selenide of antimony are potential absorber materials in devices for photovoltaic conversion of solar energy As a direct band gap semiconductor whose band gap ranges between 1.10 eV to .60 eV, it is to exhibit photovoltaic and thermoelectric characteristics which endowed the film a good potential in solar selective and a decorative coating, optical and thermoelectric cooling devices. As a matter of fact, with the type of energy band gap possessed by Sb_3Se_3 thin film, it absorbs low energy light in the visible and near infrared regions although this is affected by its deposition composition which often contributes on improving the efficiency and stabilities of its use as solar cell [8]. For instance, some groups have reported that with V-VI composition, the crystal and crystalline Sb_2Se_3 thin film has its band gap energy increased to 1.88 eV [9, 10]. Sze Reported that the conversion efficiency of Sb_2Se_3 thin film in Schottky barrier solar cells of P_t-Sb_2Se_3 [10] and n-Sb_2Se_3IP-Ge [13] structure produced structure with conversion efficiency of 5.55% and 7.3% respectively

This research paper is more oriented towards theoretical concept with regards to quest to probe into study of electromagnetic wave propagation through Antimony selenide. This is due to the fact that it is clear that the application of the thin films generally to harness solar energy and of course even other applications depend on the action of the film on electromagnetic wave propagating through it. Based on this concept, we intend to use computation from beam propagation approach

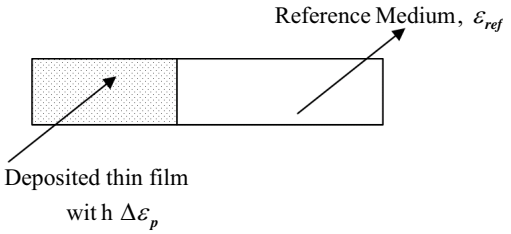

Figure 1: Deposited Sb_2Se_3 thin film model on a glass substrate, where the dielectric function is defined.

to compute the band gap and other solid state properties of Sb_2Se_3 thin film to enable one to ascertain comparatively how the computed result compares to the experimental result.

2. THEORETICAL FRAME WORK OF THE COMPUTATION

In this concept, we start by considering scalar wave equation as given below that defines general expression for wave propagating through an arbitrary medium.

$$\nabla^2\psi(r) + \omega^2\varepsilon_o\mu_o\psi(r) = 0 \quad [14\text{–}16] \tag{1}$$

But however, in this equation we introduce a perturbation that defines dielectric function consisting of reference medium, ε_{ref} representing a space without thin film and a perturbed medium $\Delta\varepsilon_p(r)$ where the thin film is deposited a defined below:

$$\varepsilon_{ref}\varepsilon_p(z) = \varepsilon_{ref} + \Delta\varepsilon(z) \tag{2}$$

where the dielectric function is defined as given below:

$$\varepsilon_p(z) = \varepsilon_{ref} + \Delta\varepsilon(z) \tag{3}$$

$$\psi\left(z, z'\right) = \int_0^{z'} G\left(z, z'\right) V\left(z'\right) \psi\left(z'\right) dz' \tag{4}$$

Given $G\left(z, z'\right)$ the Green's function specified by:

$$G\left(z, z'\right) = \frac{2}{z}\sum_{n=1}^{\infty} \frac{\sin\left(n\pi z'/z\right)}{\gamma^2 - \frac{n^2\pi^2}{z^2}} \tag{5}$$

$$V\left(z\right) = -\gamma^2\Delta\varepsilon_p\left(z\right) = -\gamma^2\left(\varepsilon_p\left(z\right) - \varepsilon_{ref}\right) \tag{6}$$

linearizing $\varepsilon_p\left(z\right)$ as follows:

$$\varepsilon_p\left(z\right) \approx \varepsilon_0 + kz + o\left(z^2\right), \tag{7}$$

We neglect higher order terms as we are dealing with thin film, where ε_0 and k are constants,

$$V\left(z\right) = -\gamma^2\Delta\varepsilon_p\left(z\right) = -\gamma^2\left(\varepsilon_p\left(z\right) - \varepsilon_{ref}\right) = -\gamma^2\left(\varepsilon_0 - \varepsilon_{ref} + kz\right) = -\gamma^2\left(\varepsilon' + kz\right) \tag{8}$$

$\varepsilon' = \varepsilon_0 - \varepsilon_{ref}$ a constant.

Furthermore, we have $\psi\left(z'\right) = \sin\left(\frac{2\pi}{\lambda}z'\right)$, hence the integral becomes:

$$\psi\left(z\right) = \int_0^{z'} \frac{2}{z}\sum_{n=1}^{\infty} \frac{\sin\left(n\pi z'/z\right)}{\gamma^2 - \frac{n^2\pi^2}{z^2}} \left(-\gamma^2\left(\varepsilon' + kz'\right)\right) \sin\left(\frac{2\pi}{\lambda}z'\right) dz' \tag{9}$$

Hence we replaced ε' by ε and write

$$I\left(z, z'\right) = -\gamma^2 \int_0^{z'} \frac{2}{z}\sum_{n=1}^{\infty} \frac{\sin\left(n\pi z'/z\right)}{\gamma^2 - \frac{n^2\pi^2}{z^2}} \left(\varepsilon + kz'\right) \sin\left(\frac{2\pi}{\lambda}z'\right) dz' \tag{10}$$

in which we obtain the integral as

$$\psi\left(z, z'\right) = -\frac{2}{z}\sum_{n=1}^{\infty} \frac{\gamma^2}{\left(\gamma^2 - \frac{n^2\pi^2}{z^2}\right)} \int_0^{z'} \sin\left(n\pi z'/z\right) \left(\varepsilon + kz'\right) \sin\left(\frac{2\pi}{\lambda}z'\right) dz' \tag{11}$$

$$\psi(z,z') = -\frac{2}{z}\sum_{n=1}^{\infty}\frac{\gamma^2}{\left(\gamma^2-\frac{n^2\pi^2}{z^2}\right)}$$
$$\times\left\{\begin{array}{l}\dfrac{\varepsilon\pi n^3\lambda^3\sin\left[\frac{(2z+n\lambda)\pi z'}{\lambda z}\right]-2\varepsilon\pi n^2\lambda^2 z\sin\left[\frac{(2z+n\lambda)\pi z'}{\lambda z}\right]-4\varepsilon\pi n\lambda z^2\sin\left[\frac{(2z+n\lambda)\pi z'}{\lambda z}\right]}{\pi^2(4z^2-n^2\lambda^2)^2}\\ +\dfrac{2\varepsilon\pi n^2\lambda^2 z\sin\left[\frac{(2z-n\lambda)\pi z'}{\lambda z}\right]-4k\pi n\lambda z^2\sin\left[\frac{(2z-n\lambda)\pi z'}{\lambda z}\right]-8\varepsilon\pi z^3\sin\left[\frac{(2z-n\lambda)\pi z'}{\lambda z}\right]}{\pi^2(4z^2-n^2\lambda^2)^2}\\ +\dfrac{8k\pi z^3 z'\sin\left[\frac{(2z+n\lambda)\pi z'}{\lambda z}\right]-8k\pi z^3 z'\sin\left[\frac{(2z-n\lambda)\pi z'}{\lambda z}\right]-4kn\lambda^2 z^2\cos\left[\frac{(2z+n\lambda)\pi z'}{\lambda z}\right]}{\pi^2(4z^2-n^2\lambda^2)^2}\\ +\dfrac{-4\varepsilon\pi n\lambda z^2\sin\left[\frac{(2z-n\lambda)\pi z'}{\lambda z}\right]+kn^2\lambda^3 z\cos\left[\frac{(2z+n\lambda)\pi z'}{\lambda z}\right]+\varepsilon\pi n^3\lambda^3\sin\left[\frac{(2z-n\lambda)\pi z'}{\lambda z}\right]}{\pi^2(4z^2-n^2\lambda^2)^2}\\ +\dfrac{k\pi n^3\lambda^3 z'\sin\left[\frac{(2z+n\lambda)\pi z'}{\lambda z}\right]+4kz^3\lambda\cos\left[\frac{(2z+n\lambda)\pi z'}{\lambda z}\right]-2k\pi n^2\lambda^2 z' z\sin\left[\frac{(2z+n\lambda)\pi z'}{\lambda z}\right]}{\pi^2(4z^2-n^2\lambda^2)^2}\\ +\dfrac{-kn^2\lambda^3 z\cos\left[\frac{(2z-n\lambda)\pi z'}{\lambda z}\right]+8\varepsilon\pi z^3\sin\left[\frac{(2z+n\lambda)\pi z'}{\lambda z}\right]-4kz^2\lambda^2 n\cos\left[\frac{(2z-n\lambda)\pi z'}{\lambda z}\right]}{\pi^2(4z^2-n^2\lambda^2)^2}\\ +\dfrac{-4kz^3\lambda\cos\left[\frac{(2z-n\lambda)\pi z'}{\lambda z}\right]-4k\pi z^2\lambda n z'\sin\left[\frac{(2z+n\lambda)\pi z'}{\lambda z}\right]-4kn\lambda^3 z^3}{\pi^2(4z^2-n^2\lambda^2)^2}\end{array}\right\}$$

3. RESULTS AND DISCUSSION

Figure 1 is the model of the thin film deposited on a glass side in which we assumed to be the perturbed medium while the portion without thin film represents the reference medium. Fig. 2 shows the optical absorbance of Sb_2Se_3 thin film which appeared is low within the UV region and increased within the optical and near-infrared region. The transmittance within 300 nm and 640 nm seemed higher as when compared to other regions though depicted lower reflectance at the said region. However, both transmittance and reflectance were seen to be high at 640 nm as in Fig. 2 and Fig. 4. The computed band gap of the thin film from the model as in Fig. 3 is 2.56 eV as compared to the experimental value which is 2.430 eV as obtained by Rodrigue-Lazeano et al. in 1999, using chemical bath deposition technique. In another experimental result using the same chemical bath deposition, the band gap was seen to be 1.62 eV while Bajpeyee used the same method and got the band gap to be 1.30 eV [2, 7]. However the prevailing discrepancy in the value of the band gap might have been as a result of the ambient temperature during which the deposition was carried out as it has been noted that annealing and the use of substrate affects the band gap. For instant the same thin film deposited on TiO_2 electrode was to depict band gap of 1.10 eV. On other hand, the discrepancy resulting from the computed band gap could be attributed to the some assumptions and some factors that were neglected during the formulation of the model equation. The behaviour of the spectral absorbance agreed with the report of Rodrigue-Lazeano et al that the thin film absorbs low energy light within visible and near-infrared regions [2]. On the other hand the transmittance and reflectance characteristics within 200 nm–300 nm confirm the observed low energy absorption within UV region. The graphs of the solid state properties were shown in Fig. 4, Fig. 6 and Fig. 7.

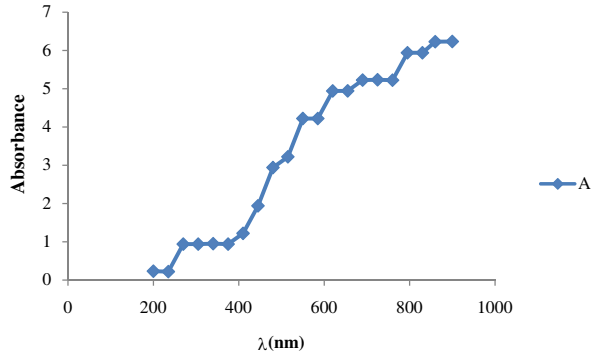

Figure 2: Graph of absorbance as a function of wavelength, λ nm for Antimony Selenide, Sb_2Se_3 thin film.

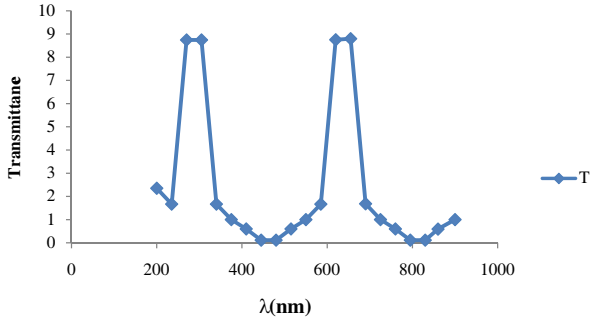

Figure 3: Transmittance vs wavelength, λ nm for Antimony Selenide, Sb_2Se_3 thin film.

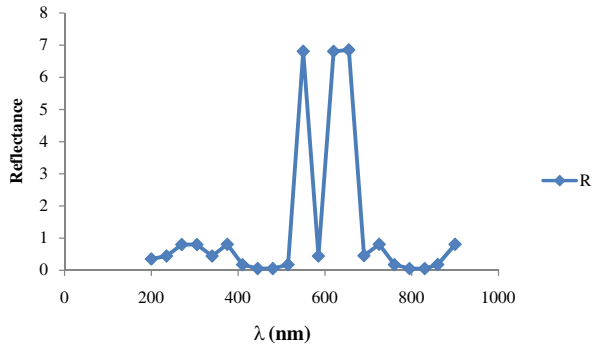

Figure 4: Reflectance vs wavelength, λ nm for Sb_2Se_3 thin film.

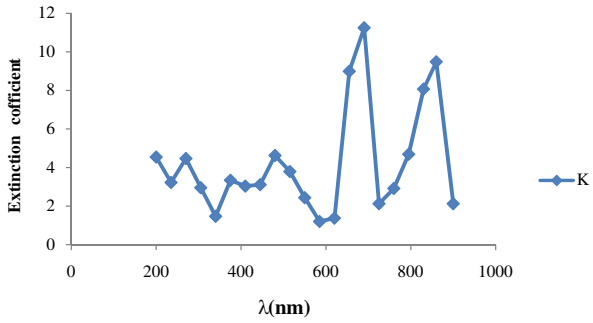

Figure 5: Extinction coefficient as a function of wavelength, λ nm for Antimony Selenide, Sb_2Se_3 thin film.

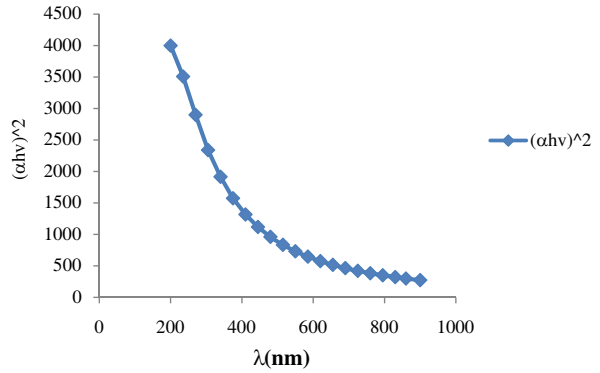

Figure 6: Graph of (αhv)^2 vs wavelength for antimony Selenide, Sb_2Se_3.

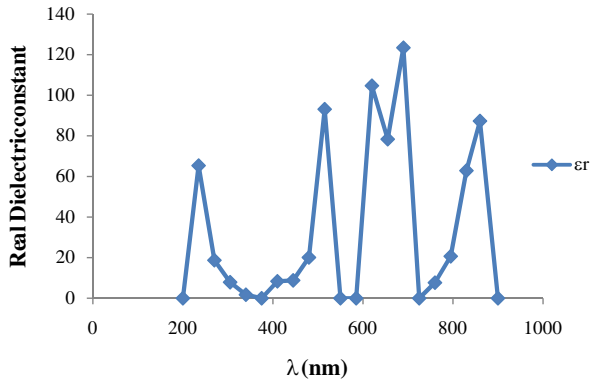

Figure 7: real dielectric constant vs wavelength, λ nm for Antimony Selenide, Sb_2Se_3 thin film.

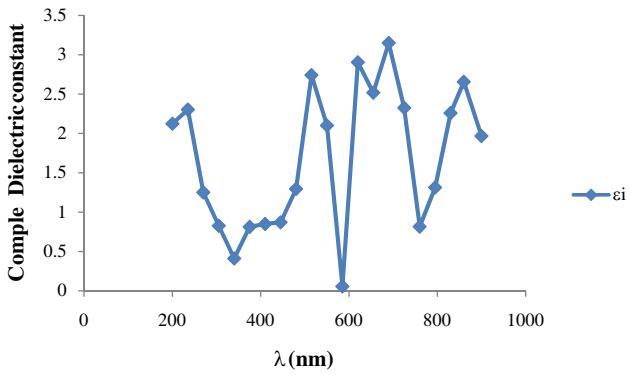

Figure 8: Imaginary dielectric constant vs wavelength, λ nm for Antimony Selenide, Sb_2Se_3 thin film.

4. CONCLUSION

An approach in the form of electromagnetic wave propagation has been employed t optimize the theoretical analysis of the optical and solid state properties of Sb_2Se_3 thin film. A model expression of wave propagating through thin film that was used in the computation was developed from scalar wave equation in conjunction with green's function technique. The data obtained from the model were used in computing the optical, solid state properties and the band gap of the thin film. Comparatively, the computed band gap apart from some approximation and assumption can be compared to the experimentally bath deposited Sb_2Se_3 thin film.

REFERENCES

1. Rajapure, K. Y., C. D Lokhande, and C. H. Bhosele, *Thin Solid Film*, Vol. 311, 114, 1997.
2. Bajpeyee, A. U., *Multilogic Sciences*, Vol. 2, No. 2, 38, 2012.

3. Yang, J., J. H. Zeng, S. H. Yu, L. Yang, Y. H. Zhang, and Y. T. Qiian, *Chem. Meter.*, Vol. 12, 2924, 2002.
4. Bao, J. C., C. Y. Tie, Z. Xu, Z. Y. Suo, Q. F. Zhou, and J. M. Hong, *Adv. Mater.*, Vol. 20, 1483, 2002.
5. Pan, Z. W., Z. R. Dac, and Z. L. Wang, *Science*, 291, Washington, D.C., 2001.
6. Dai, Z. R., D. J. L Gole, J. D. Stout, and Z. L. Wang, *J. Phys. Chem. B*, Vol. 106, 1947, 2002.
7. Owoh, B. and E. I. Ugwu, *JMME*, Vol. 1, No. 1, 38, 2009.
8. Fernandez, A. M. and M. G. Merino, *Thin Solid Films*, Vol. 366, 202–206, 2000.
9. Ritchie, L. and C. W. Kettler, *Proc SPIE*, Vol. 832, 2, 1987.
10. Nair, P. K., M. T. S. Nair, A. Fernandez, and M. Ocampo, *J.Phys. D Appl. Phys.*, Vol. 22, 829, 1989.
11. Rodriguez-Lazeano, Y. and K. N. Watanabe, *Thin Solid Films*, Vol. 493, 77–82, 2005.
12. Rodriguez-Lazeano, Y., L. Gurrero, O. G. Daza, M. T. S. Nair, and P. K. Nair, *Superficies Y Vacio*, Vol. 9, 100–103, 1999.
13. Sze, S. M., *Physics of Semiconductor Devices*, 751, Wiley, New York, 1981. and 849.
14. Dereux, J. F. O. A. and C. Girarad, *J. Opt. Soc. Am.*, Vol. 2, 1073–1081, 1994.
15. Ugwu, E. I., *Int. J. of Multi. Phsics*, Vol. 4, No. 4, 306–315, 2010.
16. Ugwu, E. I. and C. E. Okeke, *Int. J. of Multi. Physics*, Vol. 5, No. 3, 267–274.